Mar Biol
DOI 10.1007/s00227-012-1958-x

ORIGINAL PAPER

Effects of rising temperature on pelagic biogeochemistry in mesocosm systems: a comparative analysis of the AQUASHIFT Kiel experiments

Julia Wohlers-Zöllner · Antje Biermann · Anja Engel · Petra Dörge · Aleksandra M. Lewandowska · Markus von Scheibner · Ulf Riebesell

Received: 7 October 2011 / Accepted: 5 May 2012

Abstract A comparative analysis of data, obtained during four indoor-mesocosm experiments with natural spring plankton communities from the Baltic Sea, was conducted to investigate whether biogeochemical cycling is affected by an increase in water temperature of up to 6 °C above present-day conditions. In all experiments, warming stimulated in particular heterotrophic bacterial processes and had an accelerating effect on the temporal development of phytoplankton blooms. This was also mirrored in the build-up and partitioning of organic matter between particulate and dissolved phases. Thus, warming increased both the magnitude and rate of dissolved organic carbon (DOC) build-up, whereas the accumulation of particulate organic carbon (POC) and phosphorus (POP) decreased with rising temperature. In concert, the observed temperature-mediated changes in biogeochemical components suggest strong shifts in the functioning of marine pelagic food webs and the ocean's biological carbon pump, hence providing potential feedback mechanisms to Earth's climate system.

Communicated by M. Winder.

J. Wohlers-Zöllner (✉) · A. Biermann · P. Dörge · A. M. Lewandowska · U. Riebesell
Helmholtz Centre for Ocean Research Kiel (GEOMAR), Kiel, Germany
e-mail: Julia.Wohlers@bio.uib.no

Present Address:
J. Wohlers-Zöllner
University of Bergen, Bergen, Norway

A. Engel
Alfred Wegener Institute for Polar and Marine Science, Bremerhaven, Germany

Present Address:
A. Engel
Helmholtz Centre for Ocean Research Kiel (GEOMAR), Kiel, Germany

Present Address:
P. Dörge
University Medical Centre Schleswig–Holstein (UKSH), Kiel, Germany

M. von Scheibner
Leibniz Institute for Baltic Sea Research, Rostock-Warnemünde, Germany

Introduction

Earth's climate system is tightly linked with the ocean through the uptake and storage of heat (Barnett et al. 2005) and the exchange of climate-active gases, such as carbon dioxide (CO_2), at the air-sea boundary (Siegenthaler and Sarmiento 1993). While the ocean thus acts as a mitigating agent of anthropogenic climate change, it experiences major changes itself as a result of this. The absorption of heat, for instance, has led to an increase in global surface ocean water temperature (0–3,000 m) of 0.037 °C in the period 1955–1998 (Levitus et al. 2005), with a further projected rise in global surface temperature of 1–6 °C until the end of the twenty-first century (Meehl et al. 2007).

Temperature is a major environmental factor that can both directly and indirectly affect biological processes in the ocean (Boyd and Doney 2002; Sarmiento et al. 2004). While in principle, all biological processes are directly dependent on temperature; heterotrophic processes are generally expected to display a stronger sensitivity to changes in temperature than autotrophic processes (Tilzer and Dubinsky 1986; Müren et al. 2005; López-Urrutia et al. 2006). Concerning the latter, an additional pronounced dependence on light and nutrient availability is usually

Published online: 08 July 2012

assumed, thus suggesting an indirect effect of warming on autotrophic processes through temperature-induced alterations in water column stratification (Sarmiento et al. 1998; Bopp et al. 2001). In concert, the projected increase in surface ocean temperature is expected to profoundly affect the dynamics and interplay of auto- and heterotrophic processes in the pelagic marine food web and the associated biogeochemical cycling of major elements, such as carbon (C), nitrogen (N) and phosphorus (P) (Finkel et al. 2009; O'Connor et al. 2009; Riebesell et al. 2009; Morán et al. 2010).

In the framework of the 6-year programme AQUASHIFT, a series of indoor-mesocosm experiments were conducted to investigate the effects of sea surface warming on the food web dynamics of natural Baltic Sea spring plankton communities and the cycling of C, N and P within. In a synthesis of the first 3 years (i.e., 2005–2007) of AQUASHIFT experiments, in which the plankton community was exposed to a range of four temperatures (ambient and three elevated temperatures) with differing daily light doses between the years, Sommer and Lengfellner (2008) observed recurrent temperature effects on the timing of the bloom as well as on key characteristics of the phytoplankton community. Thus, the timing of the bloom peak displayed a uniform acceleration of 1–1.4 days per °C increase above ambient temperature, the composition of the autotrophic community members shifted from a diatom- to a flagellate-dominated system, and phytoplankton biomass and cell size decreased with rising temperature. In the experiments in 2008 and 2009, a different approach was chosen, exposing the plankton community to a factorial combination of two temperatures (ambient and one elevated temperature) and either three levels of daily light dose (2008) or three levels of copepod abundance (2009). While in principle showing the same effects of warming on the timing of the bloom and characteristic features of the phytoplankton community, these experiments revealed that temperature was the main driving force behind the observed acceleration of bloom dynamics, whereas daily light dose and copepod density were equally important with temperature in regulating phytoplankton biomass, average cell size and community composition (Lewandowska and Sommer 2010; Sommer and Lewandowska 2011). Moreover, Lewandowska et al. (2011) showed, using a meta-analytical approach, a direct positive effect of experimental warming on biomass-normalised primary production (PP) across all experiments, which was most pronounced at low grazing pressure and high daily light dose.

In the first of two experiments in 2006, Wohlers et al. (2009) showed that also heterotrophic processes strongly responded to rising temperature, thereby affecting the build-up, stoichiometry and the POM-DOM partitioning of organic matter. Thus, elevating the temperature by up to 6 °C above ambient conditions notably stimulated both bacterial secondary production (BSP) and community respiration already during the build-up phase of the bloom. This caused a significant reduction in the biological net drawdown of dissolved inorganic carbon, a reduced availability of particulate organic matter (POM) for sedimentation and an enhanced accumulation of dissolved organic carbon compounds. Moreover, experimental warming led to a reduced net build-up of particulate organic phosphorus (POP) and an elevated as well as accelerated accumulation of dissolved combined carbohydrates (dcCHO), thereby also affecting the stoichiometry of particulate and dissolved organic matter (Wohlers 2009; Engel et al. 2011).

Based on these findings, we reanalysed the AQUASHIFT data to test the following hypotheses:

1. Temporal dynamics of bloom development:

$H1_0$: Warming has no effect on the temporal coupling of autotrophic production and heterotrophic degradation of biomass

$H1_A$: Heterotrophic processes respond stronger to warming than autotrophic processes. Thus, increasing temperature will lead to an acceleration of heterotrophic compared to autotrophic processes, thereby altering the timing of cardinal bloom events

2. Organic matter net build-up and partitioning between particulate (i.e., POM) and dissolved phases (i.e., DOM):

$H2_0$: Warming has no effect on the balance between autotrophic production and heterotrophic degradation of biomass, with hence no changes occurring in organic matter net build-up and partitioning

$H2_A$: Heterotrophic processes respond stronger to warming than autotrophic processes. Thus, increasing temperature will stimulate the heterotrophic degradation of POM more than its autotrophic production, thereby decreasing the overall net build-up of POM. Moreover, warming will increase the partitioning of organic matter to the DOM pool through changes in algal exudation and the heterotrophic dissolution of POM

3. Organic matter elemental composition:

$H3_0$: Warming has no effect on the elemental stoichiometry of autotrophic production and heterotrophic degradation of biomass

$H3_A$: Increasing temperature stimulates the preferential recycling of nitrogen (N) and phosphorus (P) compared to carbon (C), thereby causing an increase in the C:N:P ratio of POM and DOM. Moreover, warming increases the competition for nutrients between algae and bacteria. This promotes

an enhanced exudation of dissolved organic carbon-rich compounds by algae and further increases the C:N:P ratio of DOM

To test these hypotheses and to check for recurrent patterns in the response obtained as part of the AQUASHIFT mesocosm project, we have carried out a comparative analysis of the AQUASHIFT experiments of the years 2006, 2008 and 2009. In particular, we will present results on the effects of experimental warming on the timing of cardinal bloom events, the build-up, partitioning and qualitative nature of particulate and dissolved organic matter, as well as on the dynamics of transparent exopolymeric particles (TEP).

Materials and methods

Experimental design and set-up

In the framework of the AQUASHIFT project, yearly indoor-mesocosm experiments were conducted during the spring season in the years 2005–2010. Our comparative analysis includes data of the experiments conducted in 2006 (AQ2 and AQ3), 2008 (AQ5) and 2009 (AQ6). The experiments of the years 2005, 2007 and 2010 had to be excluded from this analysis due to low-light induced problems with biomass development on the mesocosm walls in the first two studies, as well as due to a differing conceptual design of the latter study.

For the experiments AQ2 and AQ3, eight mesocosms (1,400L volume, 1 m depth, high-density polypropylene) were distributed among four temperature-controlled climate chambers, thereby allowing for a simulation of four different temperature scenarios: in situ temperature (T + 0) and temperatures elevated by 2, 4, and 6 °C above in situ temperature (T + 2, T + 4, and T + 6; see also Sommer et al. 2007 for more details).

The experiments AQ5 and AQ6 focused on the combinations of the environmental factors temperature and light intensity (AQ5), as well as temperature and overwintering copepod density (AQ6) in a factorial design. For this purpose, a total of twelve mesocosms (1400L volume, 1 m depth, HD-PP) were distributed among four climate chambers. Two chambers were run at in situ temperature T + 0, whereas the temperature of the other two chambers was increased by 6 °C above T + 0 (i.e., T + 6). The two temperature regimes were then combined with either three different light intensities (high light (HL), intermediate light (IL) and low light (LL)) or three levels of initial copepod densities (high density (HD), intermediate density (ID) and low density (LD)), simulating changes in water column mixing depth and cloud cover, as well as in the overwintering copepod population, respectively (see Table 1 for details on daily light doses and copepod abundances). All treatments were duplicated.

The ambient temperature T + 0 was derived from the decadal mean (1993–2002) spring water temperature of the investigation area Kiel Bight (Baltic Sea), yielding a value of approx. 2.5 °C. The elevated temperature scenarios T + 2, T + 4 and T + 6 were chosen according to the projections of the IPCC report for the end of the twenty-first century (Meehl et al. 2007). In the experiments AQ3, AQ5 and AQ6, the temperature of the individual mesocosms was gradually increased in the course of the experimental period to mimic the natural late winter/early spring environmental conditions, thus causing a step-wise decrease in the temperature difference between treatments by 0.25 °C per month (Sommer et al. 2007). As the algal blooms in these studies always occurred within the first 4 weeks of the experimental period, the effective water temperatures remained close to initial values, thus maintaining also the reported temperature differences between treatments.

Prior to the experiments, the mesocosms were simultaneously filled with natural seawater from Kiel Fjord (Baltic Sea), containing a natural spring plankton community as present in the Fjord at the time of filling. Due to their fragile nature, copepods were added from net catches in natural densities of 1.5–11 individuals L^{-1} (ind L^{-1}) as described in Table 1. The phytoplankton community was usually dominated by diatoms (>90 % of total algal biomass), predominantly by *Skeletonema costatum*.

Light was supplied by separate light benches above each of the mesocosms, containing 12 full-spectrum light tubes (10 solar tropic T5 Ultra (4,000 K), 2 solar nature T5 Ultra (9,000 K); JBL, Germany). The light benches were controlled by a computer simulating daily irradiance curves. In addition, a seasonal light pattern based on astronomic equations (Brock 1981) was imposed on the light system in all but one experiment (i.e., AQ2), causing a gradual increase in daily light dose over the experimental period. During AQ2, the daily light dose was kept constant over the whole experimental period. The daily light doses are given as mixed water layer values averaged over the bloom period using an attenuation coefficient of 0.25 m^{-1} (i.e., as typical for Baltic Sea winter water; Sommer and Lengfellner 2008). Due to technical changes in the light system between the first and second phase of AQUASHIFT, the daily light doses are generally higher in the second compared to the first phase with values ranging between 6.0–7.7 and 1.9–4.3 mol photons m^{-2} day^{-1}, respectively (Table 1).

In AQ2, AQ3 and AQ5, an initial copepod density of approx. 10 individuals L^{-1} (ind. L^{-1}) was aspired, but depended largely on the prevailing situation at the

Table 1 Summary of the environmental core settings during the various AQUASHIFT experiments

	AQ 2	AQ 3	AQ 5			AQ 6		
			HL	IL	LL	HD	ID	LD
Year	2006	2006	2008			2009		
ΔT	+0, +2, +4, +6	+0, +2, +4, +6	+0, +6			+0, +6		
Daily light dose	1.9	4.3	7.7	7	6	6.8		
Copepod density	5	9	8			10	4	1.5
Replicate number	2	2	2	2	2	2	2	2
$N:P_{inorg}$	30:1	15:1	18:1			17:1		

ΔT describes the net temperature difference (in °C) between the in situ (T + 0) and the elevated temperature treatments. The daily light dose value represents the average daily light dose during the bloom period (in mol photons m^{-2} day^{-1}). $N:P_{inorg}$ describes the molar ratio of dissolved inorganic nitrogen to dissolved inorganic phosphorus at the start of the experiment. The initial copepod density at the start of the experiment is given in ind. L^{-1}. All combinations of temperature, light, and copepod density were carried out in duplicate

investigation site at the time of mesocosm filling (Table 1). In AQ6, an initial copepod density of 10 (AQ6-HD), 4 (AQ6-ID) and 1.5 (AQ6-LD) ind. L^{-1} was achieved.

Dissolved inorganic nutrient concentrations varied naturally between years. In AQ2 and AQ5, 13 and 5 µmol L^{-1} nitrate (NO_3^-), respectively, were added to all mesocosms in order to obtain comparable ratios of dissolved inorganic nitrogen to phosphorus ($N:P_{inorg}$). Thus, $N:P_{inorg}$ was in all experiments above the canonical Redfield ratio of 16:1 (Table 1; Redfield et al. 1963), implying phosphorus to be the limiting nutrient.

The water in the mesocosm was gently mixed by means of a motor-driven propeller attached to the side of the mesocosms. This kept living cells and smaller particles in suspension, whereas larger particles and aggregates were allowed to sink out of the water column.

Sampling was in general carried out at least three times a week, but up to daily during bloom phases. Samples were either taken at intermediate depth by means of a silicone hose or as depth-integrated samples with a plexiglas tube that was lowered into the mesocosms and closed underneath the surface with silicon stoppers. The total sample volume taken in the course of the experiments depended on the overall duration, the frequency of sampling and the parameters investigated but was in general below 20 % of the total mesocosm volume.

Parameters

For a comparative analysis of recurrent patterns, a range of suitable parameters was chosen to describe the effect of experimental warming on food web dynamics and the associated cycling of the major elements C, N and P.

The timing of the spring plankton bloom is represented by the bloom peak (i.e., the day of maximum biomass as characterised by particulate organic carbon (POC) concentration and the onset of nutrient depletion (i.e., based on phosphate (PO_4^{3-}) concentration).

Temperature-related changes in the build-up and accumulation of particulate and dissolved organic matter are investigated through changes in the concentration of POC, POP and dissolved organic carbon (DOC; data available only for AQ2, AQ5 and AQ6). Moreover, we present data on the pool of dissolved combined carbohydrates (dcCHO), as well as on the dynamics of transparent exopolymer particles (TEP; data available only for AQ2, AQ5 and AQ6). The latter form from dissolved organic carbon compounds and can play a decisive role in the aggregation and sedimentation of particulate matter to greater depths at the end of bloom situations (Passow 2002).

Warming-related shifts in the quality of the accumulating particulate and dissolved organic matter are investigated by analysing the ratio of POC to POP (POC:POP) as well as DOC to dissolved organic phosphorus (DOP), that is, DOC:DOP (data available only for AQ2, AQ5 and AQ6).

Included in the analysis is also the average rates of algal primary production (PP; i.e., particulate and dissolved) and bacterial secondary production (BSP) to elucidate temperature-related shifts in central autotrophic and heterotrophic processes that are key drivers of biogeochemical cycling within the planktonic food web.

Measurements

Dissolved inorganic nutrient concentrations were analysed colorimetrically from filtered (cellulose acetate filters, 5 µm pore size) water samples following the protocol of Hansen and Koroleff (1999). All nutrient analyses were carried out on the day of sampling, except for samples taken during AQ6, where samples were filtered through 5-µm cellulose acetate filters (Whatman) and stored at −20 °C until analysis.

For the determination of POC and POP, 100–200 mL of sample were filtered onto pre-combusted (450 °C, 5 h) GF/F-filters (Whatman) and stored at −20 °C until analysis.

Prior to analysis on a Eurovector EuroEA-3000 elemental analyzer (Sharp 1974), POC samples were dried at 60 °C for 6 h. Particulate inorganic carbon (PIC) was not accounted for due to the absence of lithogenic carbonates and calcifying organisms. POP concentrations were determined colorimetrically after oxidation with peroxodisulphate or Oxisolv reagent (Merck), following the protocol of Hansen and Koroleff (1999).

Samples for the analysis of DOC and dissolved total carbohydrates (dtCHO) were filtered through pre-combusted (450 °C, 5 h) GF/F-filters (Whatman). The filtrate was subsequently collected in pre-combusted (450 °C, 12 h) 20-mL glass ampoules and frozen at −20 °C. DOC samples were analysed on a Shimadzu Total Organic Carbon analyser (TOC_{VCN}) using the high temperature combustion oxidation method (Qian and Mopper 1996). The concentration of dtCHO was measured spectrophotometrically using the 2,4,6-tripyridyl-s-triazine approach (Myklestad et al. 1997). Dissolved combined carbohydrates (dcCHO) were obtained by subtracting the concentration of dissolved free monosaccharides from dtCHO after acid hydrolysis (1 M HCl).

The concentration of TEP was determined colorimetrically (Passow and Alldredge 1995a). Samples were gently (<150 mbar) filtered through 0.4-µm polycarbonate filters (Whatman), stained with 1 mL of an aqueous solution of Alcian Blue (0.02 %) and stored at −20 °C until analysis. The dye was redissolved in 80 % H_2SO_4 for 3 h and the supernatant analysed on a Hitachi U-2000 spectrophotometer. All filters were prepared in duplicate. The acidic polysaccharide Gum Xanthan was used as a standard. The carbon content of TEP (µmol C L^{-1}) was calculated using a conversion factor ($f' = 0.63$; Engel 2004).

Rates of autotrophic PP and heterotrophic BSP were determined three times a week. Primary production was determined through measurements of ^{14}C-bicarbonate ($H^{14}CO_3^-$) uptake (Steemann Nielsen 1952; Gargas 1975). For this purpose, $H^{14}CO_3^-$ was added to 30 mL samples at a final activity of 4 µCi per bottle. The samples were then incubated in situ for approx. 4 h at intermediate water depth inside the respective mesocosms. All incubations were carried out in duplicate with one dark bottle serving as a blank. After incubation, sample aliquots were filtered onto 0.2-µm cellulose acetate filter in order to determine particulate primary production rates (PP_{part}). The filters were then fumed with concentrated hydrochloric acid (HCl) for 10 min in order to remove excess $H^{14}CO_3^-$, and 4 mL of scintillation cocktail (Lumagel Plus) were added. For dissolved primary production (PP_{diss}), 20 mL of filtrate received 100 µL of 1 N HCl. The filtrate was then stored in a desiccator, containing 1 N NaOH to ensure maximum outgassing of expelled CO_2, under vacuum for 8 days. Following this, a volume of 10 mL of scintillation cocktail (Aquasol) was added to each PP_{diss} sample. Finally, all samples were radio-assayed on a Packard TriCarb scintillation counter. Daily PP (µg C L^{-1} day^{-1}) was calculated by multiplying the obtained production rates with a light factor (total amount of light throughout the day divided by the amount of light received during the incubation).

Bacterial secondary production was assessed by measuring the incorporation of ^{3}H-leucine (^{3}H-leu; only AQ2, 5), ^{14}C-leucine (^{14}C-leu; only AQ6) or ^{3}H-methyl-thymidine (^{3}H-thy; only AQ3), following the protocols by Simon and Azam (1989) and Fuhrman and Azam (1982). ^{3}H-leu (specific activity: 160 µCi $nmol^{-1}$), ^{14}C-leu (specific activity: 306 mCi $mmol^{-1}$) and ^{3}H-thy (specific activity: 63 µCi $nmol^{-1}$) were added to the samples at final concentrations of 103, 97.8 and 8 nmol L^{-1}, respectively. The samples were dark-incubated at in situ temperature (i.e., in the respective climate chambers) for 1.5–3 h. Incubation was terminated by adding formaldehyde (1 % v/v). A sample volume of 5–10 mL was then filtered onto 0.2-µm polycarbonate membrane filters (Poretics®). The filters were subsequently rinsed with ice cold 5 % TCA solution before being radio-assayed in 4 mL of scintillation cocktail (Lumagel Plus) on a Packard TriCarb scintillation counter. All incubations were carried out in triplicate. A formalin-killed sample was used to correct for background absorption of radioactivity. To convert the incorporation of ^{3}H-leu and ^{3}H-thy into carbon production (µg C L^{-1} h^{-1}), a theoretical conversion factor of 3.1 kg C mol^{-1} leucine (Simon and Azam 1989) and an empirically determined conversion factor of 30.87 kg C mol^{-1} thymidine (Breithaupt 2009), respectively, were used. The daily carbon production rates (µg C L^{-1} day^{-1}) were then calculated, assuming that bacterial production rates were constant throughout the day.

Calculations

For direct comparison of the different experiments, we defined cardinal points of the temporal bloom development, such as the beginning and end of the bloom period, as well as the onset of nutrient depletion (Fig. 1). The bloom period to be included in the analysis was determined by calculating the natural logarithm of POC concentration (ln[POC]; Fig. 1). During exponential growth and decay, ln[POC] should scale linearly with time. We took advantage of this for defining the first day during the build-up phase as well as the last day during the degradation phase by applying general linear regression models to ln[POC] data (for the build-up phase from the approximate onset of increasing ln[POC] to maximum ln[POC] and for the degradation phase from maximum ln[POC] to the approximate minimum ln[POC]; see also Fig. 1). The range of data yielding the best fit in terms of r^2 was chosen to be the best

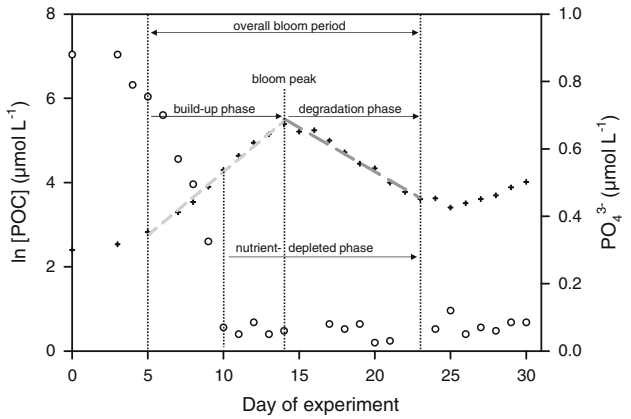

Fig. 1 Schematic representation of a characteristic development of POC concentration in the course of an algal bloom, illustrating relevant definitions of cardinal bloom events. The *symbols* represent exemplary logarithmic POC concentration (ln[POC]; in µmol C L^{-1}; *cross symbol*) and dissolved inorganic phosphate concentration (PO_4^{3-}; in µmol L^{-1}; *open circles*) from one of the AQUASHIFT studies (AQ2). The *dashed lines* represent the linear regression models that were fitted to the build-up phase (*light grey*) and the degradation phase (*dark grey*) of the bloom

representative for defining the respective build-up and degradation phase. The day of bloom peak was defined as the day of maximum POC concentration. Another important time point during bloom development is the onset of nutrient depletion, which was defined as the first day where PO_4^{3-} concentration fell below the detection limit of 0.05 µmol L^{-1} (Fig. 1).

Following the above criteria, the average build-up of POC (POC_{mean}), POP (POP_{mean}) and DOC (DOC_{mean}) was determined by calculating their geometric mean over the defined bloom period. For comparison of organic matter quality between treatments, the geometric mean of the ratios of POC to POP ($POC:POP_{mean}$) and DOC to DOP ($DOC:DOP_{mean}$) was calculated for the period from nutrient depletion onward until the last day of the bloom period. With regard to the accumulation of dissolved organic components and the elemental composition of organic matter, the onset of nutrient depletion is generally a cardinal time point in bloom situations, as it may trigger the exudation and accumulation of dissolved carbon-rich material (Norrman et al. 1995; Thingstad et al. 1997; Van den Meersche et al. 2004). This often leads to strong deviations in organic matter stoichiometry and may hence affect food web dynamics.

The rate of increase in DOC concentration (DOC_{slope}) and dcCHO concentration ($dcCHO_{slope}$) was determined by applying a general linear regression model for the time period from nutrient depletion until the end of the bloom period. For the analysis of TEP dynamics, both the geometric mean concentration during the full bloom period (TEP_{mean}) as well as the maximum TEP concentration (TEP_{max}), which was reached at approximately 11 days (AQ2) and 20 days (AQ5 and AQ6) after the bloom peak, were determined.

For the average rates of algal primary production (PP_{part} and PP_{diss}) and heterotrophic bacterial production (BSP_{mean}), a geometric mean was calculated over the bloom period. Additionally, the average BSP at the time of maximum [POC] was calculated ($BSP_{bloom\ peak}$).

Statistical analysis

The primary goal of our comparative analysis is to identify and describe recurrent trends in the response of important biogeochemical parameters to experimental warming across a series of mesocosm experiments with natural Baltic Sea plankton communities. In order to provide objective criteria to describe the direction and amplitude of these trends with increasing temperature, two statistical strategies were pursued, depending on the specific experimental set-up (i.e., with experimental warming as the sole environmental stressor or in factorial combination with daily light dose or copepod density). For AQ2 and AQ3, where the plankton communities were exposed to a range of four temperatures, the parameter responses to rising temperature were investigated using linear regression models (STATISTICA, Statsoft). For AQ5 and AQ6, where a factorial combination of three light doses or three copepod densities with two temperature regimes was applied, the parameter responses were investigated through general linear models (GLM; STATISTICA, Statsoft) with temperature as a categorical factor and light dose or copepod density as a continuous factor. For cases of a significant single effect of light dose or copepod density on a specific parameter, a separate linear regression of this response parameter (y) versus light dose or copepod density (x) was calculated. For all analyses, a significance level of $P < 0.05$ was applied.

In order to determine the overall effect of experimental warming on the various parameters across all experiments, the ln-transformed response ratio (*Ln*RR) was calculated for the relevant biogeochemical parameters for each experiment with

$$LnRR = \ln(M_E) - \ln(M_C),$$

where M_E and M_C are the mean values of observations in the elevated (T + 6) and ambient temperature treatments (T + 0), respectively. Following this, an overall mean effect size was calculated across all studies, including the 95 % confidence interval (CI). A mean effect size of zero indicates that temperature had no or not a consistent effect on the investigated parameter, whereas positive and negative values indicate consistent temperature effects. Following the meta-analysis approach of Kroeker et al. (2010),

the effect size was considered to be significant ($\alpha = 0.05$) when the CI did not overlap with zero.

Results

Timing of biomass maximum and nutrient exhaustion

The timing of the bloom peak ($bloom_{peak}$), as characterised by maximum POC accumulation, showed a significant ($P < 0.01$) forward shift with increasing temperature in all experiments, ranging between 1.0 and 2.8 days °C^{-1} (Tables 2, 3, 4, 5; Fig. 2). In AQ5 also, increasing daily light dose significantly accelerated the timing of the bloom peak by 2.1 days per mol photons m^{-2} day^{-1} ($P < 0.01$; Table 4; Fig. 2), whereas changes in copepod density had no notable effect during AQ6 ($P = 0.3$; Table 2).

Similarly, the onset of exhaustion of the limiting nutrient PO_4^{3-} ($PO_4^{3-}{}_{depl}$; Tables 2, 3, 4, 5; Fig. 2) occurred earlier by 0.3–2.3 days °C^{-1} ($P < 0.01$) across all studies. In comparison, increasing daily light dose or copepod density did not alter the timing of $PO_4^{3-}{}_{depl}$ ($P \geq 0.6$; Tables 4, 5).

Algal primary production and bacterial secondary production

Both bloom-averaged particulate and dissolved primary production showed a mostly negative but overall weak response to rising temperature throughout all experiments. Thus, particulate PP_{mean} displayed a significant negative trend with increasing temperature only in AQ6 ($P < 0.05$; Table 5; Fig. 2), whereas AQ2 showed a significant negative effect of experimental warming on dissolved PP_{mean} ($P < 0.01$; Table 2; Fig. 2). Copepod density affected particulate PP_{mean} significantly during the AQ6 study, causing a decrease with increasing grazer density ($P < 0.05$; Table 5; Fig. 2).

In contrast, BSP rates showed a mostly positive response to increasing temperature, with a significant stimulation of BSP_{mean} by warming in three out of four studies (AQ3, AQ5 and AQ6; $P < 0.01$; Tables 3, 4, 5; Fig. 2). Interestingly, this effect became already visible when looking at an earlier stage of the bloom period. Thus, BSP rates measured at the time of maximum POC accumulation ($BSP_{bloom\ peak}$) also displayed a significant positive trend with rising temperature in three out of four studies (AQ2, AQ5 and AQ6; $P < 0.01$; Tables 2, 4, 5; Fig. 2). In contrast, daily light dose and copepod density had no significant effect on both BSP_{mean} and $BSP_{bloom\ peak}$ across all studies ($P \geq 0.09$; Tables 4, 5; Fig. 2).

Build-up of particulate and dissolved organic matter

The average build-up of POC during the bloom period showed a variable response to increasing temperature throughout all experiments. While no effect of warming could be observed in AQ2 and AQ6, POC_{mean} significantly decreased with rising temperature by 7.3 and 17.0 µmol C L^{-1} per °C in AQ3 and AQ5 ($P < 0.01$, Tables 3, 4; Fig. 2), respectively. Changes in daily light dose and copepod density did not affect POC_{mean} ($P \geq 0.15$, Tables 4, 5; Fig. 2). Similarly, the average build-up of POP showed a significant negative trend with increasing temperature in AQ2 and AQ5 ($P < 0.001$, Tables 2, 4; Fig. 2). Warming also negatively influenced

Table 2 Summary of results for AQ2

Dependent variable	Slope	*P*	F	r^2
$Bloom_{peak}$ (day of experiment)	−1.4	0.0020	27.53	0.82
$PO_4^{3-}{}_{depl}$ (day of experiment)	−0.69	0.0009	14.71	0.71
part. PP_{mean} (µg C L^{-1} day^{-1})	−7.12	0.2640	1.51	0.20
diss. PP_{mean} (µg C L^{-1} day^{-1})	−0.71	0.0019	27.71	0.82
BSP_{mean} (µg C L^{-1} day^{-1})	0.53	0.5220	0.46	0.07
$BSP_{bloom\ peak}$ (µg C L^{-1} day^{-1})	4.63	0.0070	15.47	0.72
POC_{mean} (µmol C L^{-1})	−3.39	0.2400	1.72	0.22
POP_{mean} (µmol P L^{-1})	−0.012	0.0005	45.44	0.88
DOC_{mean} (µmol C L^{-1})	5.70	0.0219	9.42	0.61
$dcCHO_{mean}$ (µmol C L^{-1})	2.36	0.2500	1.63	0.21
DOC_{slope} (µmol C L^{-1} day^{-1})	0.73	0.0100	13.62	0.69
$dcCHO_{slope}$ (µmol C L^{-1} day^{-1})	0.68	0.0008	38.12	0.86
$POC:POP_{mean}$ (mol:mol)	−0.11	0.9900	0.00	0.00
$DOC:DOP_{mean}$ (mol:mol)	11.20	0.5400	0.42	0.07
TEP_{mean} (µmol C L^{-1})	−0.264	0.3340	1.10	0.16
TEP_{max} (µmol C L^{-1})	1.09	0.0474	6.18	0.51

A linear regression model was applied to all data sets ($n = 8$; $df = 1$)

Table 3 Summary of results for AQ3

Dependent variable	Slope	*P*	F	r^2
$Bloom_{peak}$ (day of experiment)	−0.98	0.0040	21.04	0.78
$PO_4^{3-}{}_{depl}$ (day of experiment)	−0.34	0.0070	16.37	0.73
part. PP_{mean} (µg C L^{-1} day^{-1})	−2.79	0.1955	2.12	0.26
diss. PP_{mean} (µg C L^{-1} day^{-1})	−0.66	0.0507	5.94	0.50
BSP_{mean} (µg C L^{-1} day^{-1})	1.52	0.0010	31.44	0.84
$BSP_{bloom\ peak}$ (µg C L^{-1} day^{-1})	0.04	0.9640	0.00	0.00
POC_{mean} (µmol C L^{-1})	−7.31	0.0047	19.18	0.76
POP_{mean} (µmol P L^{-1})	−0.013	0.0940	3.95	0.40
$POC:POP_{mean}$ (mol:mol)	−14.227	0.0040	20.32	0.77

A linear regression model was applied to all data sets ($n = 8$; $df = 1$)

Table 4 Summary of results for AQ5

Dependent variable	Temperature		Daily light dose		P model	*F* model	r^2
	b	P	b	P			
$Bloom_{peak}$ (day of experiment)	−2.25	0.0011	−2.08	0.0075	0.0009	17.12	0.79
$PO_4^{3-}{}_{depl}$ (day of experiment)	−1.00	0.0008	−0.56	0.0566	0.0014	14.79	0.77
part. PP_{mean} (µg C L^{-1} day^{-1})	−3.97	0.1500	3.67	0.2800	0.1600	2.30	0.34
diss. PP_{mean} (µg C L^{-1} day^{-1})	−0.46	0.1379	0.20	0.5978	0.2791	1.48	0.25
BSP_{mean} (µg C L^{-1} day^{-1})	3.75	0.0045	0.57	0.6600	0.0115	7.63	0.63
$BSP_{bloom\ peak}$ (µg C L^{-1} day^{-1})	10.61	0.0001	−4.09	0.0900	0.0004	21.49	0.83
POC_{mean} (µmol C L^{-1})	−16.98	0.0002	3.08	0.4200	0.0005	19.73	0.81
POP_{mean} (µmol P L^{-1})	−0.04	0.0001	0.01	0.5800	0.0004	21.75	0.93
DOC_{mean} (µmol C L^{-1})	17.48	0.0032	−8.98	0.1400	0.0090	8.33	0.65
$dcCHO_{mean}$ (µmol C L^{-1})	4.37	0.0600	−4.44	0.1200	0.0700	3.67	0.45
DOC_{slope} (µmol C L^{-1} day^{-1})	2.67	0.0005	−0.75	0.2800	0.0018	13.78	0.75
$dcCHO_{slope}$ (µmol C L^{-1} day^{-1})	1.25	0.0014	−1.15	0.0099	0.0012	15.47	0.77
$POC:POP_{mean}$ (mol:mol)	−13.44	0.0900	3.25	0.7300	0.1800	2.05	0.31
$DOC:DOP_{mean}$ (mol:mol)	−15.29	0.6400	43.17	0.3100	0.4800	0.80	0.15
TEP_{mean} (µmol C L^{-1})	4.05	0.0001	−0.93	0.2900	0.0005	20.38	0.82
TEP_{max} (µmol C L^{-1})	6.85	0.0018	−2.72	0.2100	0.0054	9.83	0.69

A general linear model was applied to all data sets with temperature (in °C) as categorical factor and daily light dose (in mol photons m^{-2} day^{-1}) as continuous factor ($n = 12$; $df = 2$)

POP_{mean} in the AQ3 and AQ6 studies, but the effect was slightly insignificant ($P \leq 0.1$; Tables 3, 5; Fig. 2). POP_{mean} remained unaffected by both daily light dose and copepod density ($P \geq 0.12$; Tables 4, 5; Fig. 2).

In contrast to the build-up of particulate organic matter, the average accumulation of DOC throughout the bloom period displayed a significant positive trend with rising temperature in two out of three studies (AQ2: $P < 0.05$, AQ5: $P < 0.01$; no data available for AQ3; Tables 2, 4; Fig. 2). No effect of daily light dose in the AQ5 study or of temperature and copepod density in AQ6 was observed ($P \geq 0.14$; Tables 4, 5; Fig. 2). In line with this, also the rate at which DOC accumulated (DOC_{slope}) showed a significant positive trend with increasing temperature in AQ2 ($P < 0.05$; Table 2; Fig. 2) and AQ5 ($P < 0.001$; Table 4; Fig. 2).

Looking at a specific compartment of DOC, that is, the pool of dcCHO, revealed a more complex picture. Thus, the $dcCHO_{mean}$ displayed no significant response to any of the tested environmental stressors across all three studies (Fig. 2). In contrast, the rate of dcCHO accumulation ($dcCHO_{slope}$) responded positively to warming in two out of three studies (AQ2: $P < 0.001$, AQ5: $P < 0.01$; Tables 2, 4; Fig. 2), whereas increasing light dose and copepod density had a significant negative effect on $dcCHO_{slope}$ in AQ5 ($P < 0.01$; Table 4; Fig. 2) and AQ6 ($P < 0.05$; Tables 5, 6; Fig. 2).

TEP dynamics

The dynamics of TEP concentration during and after the bloom period showed two divergent patterns in the

Table 5 Summary of results for AQ6

Dependent variable	Temperature		Copepod density		P model	*F* model	r^2
	b	P	b	P			
$Bloom_{peak}$ (day of experiment)	−2.83	0.0001	−0.13	0.2993	0.0003	23.67	0.84
$PO_4^{3-}{}_{depl}$ (day of experiment)	−2.33	0.0000	−0.03	0.6869	0.0001	34.66	0.89
part. PP_{mean} (µg C L^{-1} day^{-1})	−15.79	0.0119	−3.56	0.0326	0.0097	8.10	0.64
diss. PP_{mean} (µg C L^{-1} day^{-1})	0.06	0.9841	0.51	0.5664	0.1773	0.84	0.04
BSP_{mean} (µg C L^{-1} day^{-1})	9.71	0.0045	−3.65	0.2800	0.0110	7.74	0.63
$BSP_{bloom\ peak}$ (µg C L^{-1} day^{-1})	18.29	0.0012	−9.66	0.0906	0.0024	13.03	0.74
POC_{mean} (µmol C L^{-1})	4.91	0.4300	−2.59	0.1500	0.2600	1.55	0.26
POP_{mean} (µmol P L^{-1})	−0.02	0.0500	0.01	0.1200	0.0600	3.97	0.47
DOC_{mean} (µmol C L^{-1})	−10.99	0.2400	−0.86	0.7300	0.4500	0.86	0.16
$dcCHO_{mean}$ (µmol C L^{-1})	−5.41	0.2700	−0.98	0.4700	0.4100	0.97	0.18
DOC_{slope} (µmol C L^{-1} day^{-1})	−0.28	0.4200	−0.21	0.5400	0.5900	0.56	0.11
$dcCHO_{slope}$ (µmol C L^{-1} day^{-1})	0.34	0.3600	−0.26	0.0260	0.0600	4.01	0.47
$POC{:}POP_{mean}$ (mol:mol)	31.73	0.0600	−12.09	0.0176	0.0180	6.49	0.59
$DOC{:}DOP_{mean}$ (mol:mol)	27.67	0.6600	−7.02	0.6900	0.8300	0.19	0.04
TEP_{mean} (µmol C L^{-1})	0.19	0.2200	0.14	0.0079	0.0170	6.64	0.60
TEP_{max} (µmol C L^{-1})	7.47	0.0144	−0.49	0.5000	0.0340	4.82	0.52

A general linear model was applied to all data sets with temperature (in °C) as categorical factor and copepod density (in ind. L^{-1}) as continuous factor ($n = 12$; $df = 2$)

different experiments. The first modus was characterised by low and temperature-independent TEP concentrations during the algal bloom phase, followed by a steep increase in TEP during the late post-bloom phase, which only occurred in the elevated temperature treatments. This pattern was observed in the studies AQ2 and AQ6. The second modus was characterised by a substantial increase in TEP already during the algal bloom phase. While the concentration of TEP thereafter decreased in the in situ temperature treatments, it stagnated or even increased at elevated temperature. Study AQ5 represents an example of this pattern.

In line with these observations, a significant positive trend of TEP_{mean} with rising temperature was observed only in AQ 5 ($P < 0.001$; Table 4; Fig. 2), whereas TEP_{mean} did not respond significantly to warming in the AQ2 and AQ6 studies ($P \geq 0.22$; Tables 2, 5; Fig. 2). In AQ6, TEP_{mean} decreased significantly with increasing grazer density ($P < 0.05$; Tables 5, 6; Fig. 2).

TEP_{max}, on the other hand, displayed a significant positive trend with rising temperature in all studies (AQ2: $P < 0.05$; AQ5: $P < 0.01$; AQ6: $P < 0.05$; Tables 2, 4, 5; Fig. 2), whereas changes in light dose and copepod density had no apparent effect on this parameter ($P \geq 0.21$; Tables 4, 5; Fig. 2).

Elemental stoichiometry of POM and DOM

The average ratio of POC to POP showed a significant negative trend with rising temperature only in one out of four studies (AQ3: $P < 0.01$, Table 3; Fig. 2). A significant negative response of $POC{:}POP_{mean}$ was also observed with increasing copepod density in AQ6 ($P < 0.05$; Tables 5, 6; Fig. 2). $DOC{:}DOP_{mean}$ did not show a significant response to any of the environmental stressors: temperature, light or grazing pressure ($P \geq 0.3$; Tables 2, 3, 4, 5; Fig. 2).

Meta-analysis

Mean effect sizes were calculated for all available parameters (Table 7; Fig. 3). The timing of the bloom peak as well as the onset of PO_4^{3-} depletion were clearly accelerated by experimental warming, with low variance in mean effect size across all studies. The mean effect size of both particulate and dissolved PP_{mean} showed a tendency to reduced autotrophic production at elevated temperature, although the variance between studies was high for dissolved PP_{mean}. In contrast, bloom-averaged heterotrophic bacterial production was clearly stimulated by warming across all studies, with an even stronger response already at the time of the biomass peak (i.e., $BSP_{bloom\ peak}$).

As a consequence of these changes in the balance between autotrophic and heterotrophic processes with an increase in temperature of 6 °C, marked alterations in the build-up and partitioning of organic matter were observed across studies. Both the average accumulation of POC and POP throughout the bloom period showed a negative tendency with rising temperature, which, in the case of

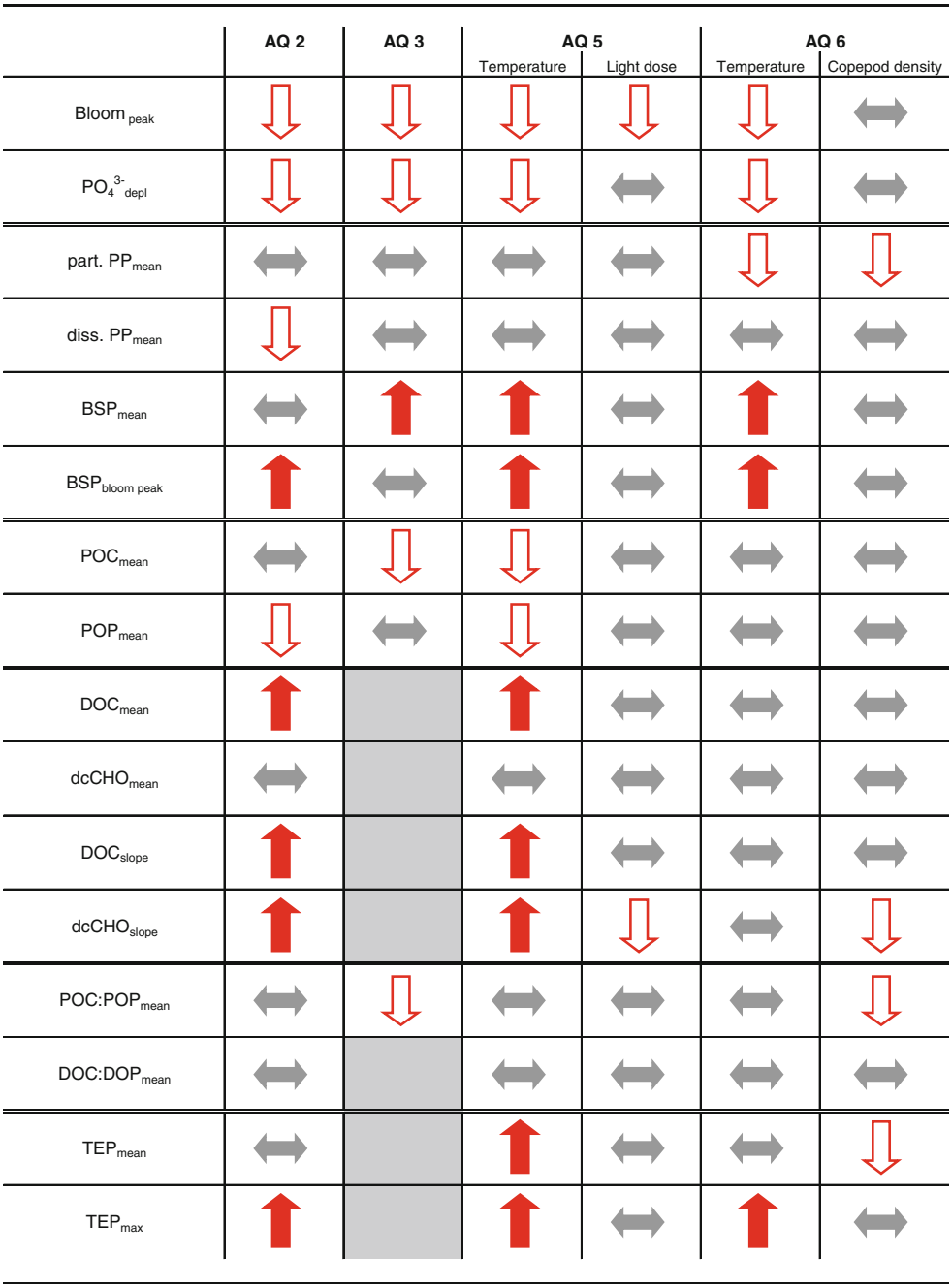

Fig. 2 Synthesis of observed effects of experimental warming by up to 6 °C above ambient temperature, changes in daily light dose (only AQ5), and overwintering copepod density (AQ6) on selected biogeochemical parameters during the AQUASHIFT experiments. The *red upward/filled* and *downward/empty arrows* denote significant ($P < 0.05$) positive or negative effects of the investigated environmental stressors on individual parameters. *Grey horizontal arrows* denote insignificant results. *Grey filled areas* denote parameters where no data were available

POP_{mean}, was clearly significant. In contrast, both the average build-up of DOC and of dcCHO did not respond notably to experimental warming, although the latter parameter showed a fairly high variability between studies. Looking at the rate of increase in DOC and dcCHO, however, showed a clear positive trend with increasing temperature. Due to a high variability of DOC_{slope}, this was, however, only significant in the case of $dcCHO_{slope}$.

The mean effect size of $POC:POP_{mean}$ showed a very weak tendency to decrease with rising temperature, but overall the elemental stoichiometry of POM and DOM did not show a pronounced response to warming across the AQUASHIFT studies. The mean effect sizes of both TEP_{mean} and TEP_{max} showed a tendency to increasing TEP accumulation with rising temperature across studies was significant only for TEP_{max}.

Discussion

Despite substantial differences in environmental conditions (e.g., daily light dose, grazer density and plankton

Table 6 Linear regression analysis of selected variables versus copepod density (AQ6), separated for the two temperature regimes T + 0 and T + 6 ($n = 6$; $df = 1$)

Dependent variable	Slope	P	F	r^2
At T + 0 °C				
$POC:POP_{mean}$ (mol:mol)	−2.8	0.580	0.36	0.08
$dcCHO_{slope}$ (µmol C L^{-1} day^{-1})	−0.16	0.34	1.19	0.23
TEP_{mean} (µmol C L^{-1})	0.13	0.15	3.28	0.45
At T + 6 °C				
$POC:POP_{mean}$ (mol:mol)	−21.3	0.004	34.55	0.90
$dcCHO_{slope}$ (µmol C L^{-1} day^{-1})	−0.36	0.048	7.94	0.66
TEP_{mean} (µmol C L^{-1})	0.142	0.033	10.42	0.72

Table 7 Summary of the meta-analysis results on the effect of increasing temperature on selected biogeochemical parameters

Experiment	$Bloom_{peak}$	$PO_4^{3-}{}_{depl}$	part. PP_{mean}	diss. PP_{mean}	BSP_{mean}	$BSP_{bloom\ peak}$	POC_{mean}	POP_{mean}
AQ2—IL, ID	−0.39	−0.21	−0.20	−0.52	0.08	0.81	−0.25	−0.19
AQ3—HL, HD	−0.62	−0.55	−0.28	−1.81	0.51	−0.04	−0.59	−0.24
AQ5—HL, HD	−0.37	−0.21	−0.27	−0.50	0.33	0.60	−0.36	−0.23
AQ5—IL, HD	−0.22	−0.13	0.02	0.13	0.23	0.69	−0.33	−0.13
AQ5—LL, HD	−0.14	0.00	−0.42	−0.38	0.20	0.75	−0.34	−0.19
AQ6—IL, HD	−0.36	−0.27	−0.29	−0.09	0.42	0.84	−0.11	−0.16
AQ6—IL, ID	−0.41	−0.45	−0.33	0.22	0.25	0.55	0.02	−0.04
AQ6—IL, LD	−0.33	−0.47	−0.38	−0.17	0.66	0.53	0.35	−0.10
Mean all	−0.35	−0.28	−0.27	−0.39	0.34	0.59	−0.20	−0.16
SD	0.14	0.19	0.14	0.63	0.19	0.28	0.29	0.07
Variance	0.02	0.04	0.02	0.40	0.03	0.08	0.08	0.00
+95 % CI	−0.24	−0.13	−0.15	0.14	0.49	0.82	0.04	−0.10
−95 % CI	−0.47	−0.44	−0.38	−0.92	0.18	0.36	−0.44	−0.21
Experiment	DOC_{mean}	$dcCHO_{mean}$	DOC_{slope}	$dcCHO_{slope}$	$POC:POP_{mean}$	$DOC:DOP_{mean}$	TEP_{mean}	TEP_{max}
AQ2—IL, ID	0.15	0.20	0.90	0.90	−0.02	0.11	−0.34	0.51
AQ3—HL, HD					−0.39			
AQ5—HL, HD	0.11	0.19	0.72	0.37	−0.12	−0.08	0.27	0.37
AQ5—IL, HD	0.05	−0.02	0.50	0.85	−0.13	−0.03	0.32	0.34
AQ5—LL, HD	0.16	0.51	0.81	0.94	−0.04	0.03	0.43	0.74
AQ6—IL, HD	−0.15	−0.92	−1.02	−0.19	−0.03	−0.09	0.09	2.25
AQ6—IL, ID	−0.09	−0.31	0.00	0.30	0.07	0.03	0.06	0.64
AQ6—IL, LD	0.04	0.22	0.28	0.35	0.58	0.18	0.08	0.89
Mean all	0.04	−0.02	0.31	0.50	−0.01	0.02	0.13	0.82
SD	0.12	0.47	0.67	0.42	0.28	0.10	0.25	0.66
Variance	0.01	0.22	0.45	0.17	0.08	0.01	0.06	0.44
+95 % CI	0.15	0.42	0.93	0.89	0.22	0.11	0.36	1.43
−95 % CI	−0.07	−0.45	−0.30	0.12	−0.24	−0.07	−0.10	0.21

Blank entries denote parameters where no data were available

community composition), our analysis showed several recurring trends of biogeochemically relevant parameters with a rise in temperature of up to 6 °C (Figs. 2, 3). These will be discussed in detail within the context of our working hypotheses.

Temporal dynamics of bloom development

Concerning the timing of cardinal plankton bloom events, such as the peak of the bloom and the onset of nutrient depletion, a consistent acceleration by on average 1.9 and

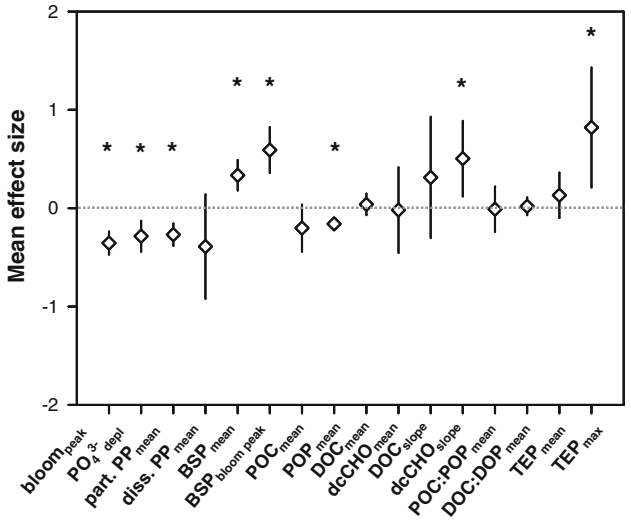

Fig. 3 Variation in the overall response of various biogeochemical parameters to an increase in water temperature of 6 °C. *Symbols* represent the mean effect sizes. The *error bars* denote the individual ±95 % confidence intervals. The *zero line* indicates the absence of a temperature effect. *Asterisk* indicates accepted significance

1.1 days $°C^{-1}$, respectively, was observed across all 4 AQUASHIFT studies. Similarly, also increasing light dose led to a significantly earlier bloom peak in the AQ5 study (Fig. 2; Table 5; Lewandowska and Sommer 2010). This also likely indicates a temporal acceleration of autotrophic processes.

The significance of this temperature-mediated forward shift in bloom timing for natural environments, however, may be less clear. Thus, the onset of the spring bloom naturally shows a high inter-annual variability of up to several weeks due to its dependence on various environmental factors, such as light availability and water column stratification. While data from a modelling study in the North-Western North Sea (Sharples et al. 2006) showed that air temperature was the main controlling factor for water column stratification and spring bloom timing, long-term monitoring studies in the North Sea could not show a significant effect of temperature on spring bloom timing (Edwards and Richardson 2004; Wiltshire and Manly 2004).

The strong stimulation of BSP by warming already at the time of the biomass peak in 3 out of 4 studies (Fig. 2) suggests, however, a closer temporal coupling of autotrophic and heterotrophic processes with increasing temperature.

Organic matter net build-up and its partitioning between particulate and dissolved phases

The data on POC and POP build-up showed significant trends towards a lower net accumulation of POM at elevated temperature in 2 of 4 studies for each parameter (Fig. 2). In the case of POP, the trend was comparable, but slightly insignificant also in a third study. Concerning the overall effect of rising temperature on these parameters, the mean effect size yielded a consistent negative trend for the net build-up of POP, whereas it remained inconclusive in the case of POC due to a high variance between studies.

In theory, the lower net build-up of POP may be caused both by a decline in the photosynthetic production of organic matter and/or an increase in its heterotrophic consumption. Here, the available data on algal primary production and BSP rates likely indicate a combination of both mechanisms. Thus, the mean effect size of particulate PP showed an overall consistent negative trend with an increase in temperature of 6 °C (Fig. 3). Looking at the individual studies, however, revealed a significant temperature effect in only one study (AQ6; Fig. 2). In line with this, Lewandowska et al. (2011) reported in a recent analysis, dealing specifically with the effect of experimental warming on algal PP in the AQUASHIFT studies, an insignificant response of particulate PP to increasing temperature. These minor differences in the temperature response of algal PP between our analysis and that of Lewandowska and co-workers likely originate from differences in the experimental time periods that were included in the calculations. In contrast to the algal processes, both BSP_{mean} and $BSP_{bloom\ peak}$ were significantly stimulated by experimental warming in 3 of 4 studies (Fig. 2), thus yielding consistent and strong positive trends with increasing temperature (Fig. 3).

Considering the dynamics in the dissolved fraction of organic matter, a significantly faster and higher increase in the accumulation of DOC was observed at elevated compared to ambient temperature in 2 of 3 studies (AQ2; AQ5; Fig. 2). Likewise, also the rate of increase in dcCHO was significantly stimulated by warming in 2 of 3 studies. Due to contrary results for DOC_{mean} and DOC_{slope} in AQ6, however, only the mean effect size of $dcCHO_{slope}$ yielded a consistent positive trend with increasing temperature across studies (Fig. 3).

The accumulation of dissolved organic carbon species during bloom events has often been observed with the onset of nutrient depletion (Copin and Avril 1993) and is generally attributed to the overflow of algal photosynthates (Engel et al. 2002; Schartau et al. 2007). In line with this, the analysis of the composition of the dcCHO pool for the AQ2 experiment showed a predominant accumulation of combined glucose (Engel et al. 2011)that is a main storage component of algal cells. While a stimulating effect of warming on primary production and the release of carbon-rich compounds has also been reported from other studies (Verity 1981; Davison 1991; Wolfstein et al. 2002; Morán et al. 2006; Claquin et al. 2008), the here determined rates

of dissolved PP, however, either showed a negative (AQ2; Fig. 2) or no response to rising temperature (AQ5, AQ6; Fig. 2). Besides phytoplankton, also bacteria contribute to DOC accumulation, for instance by releasing cell-surrounding material during active growth or through modification of DOM compounds (Azam 1998; Stoderegger and Herndl 1998; Ogawa et al. 2001; Kawasaki and Benner 2006; Kujawinski 2011). As the heterotrophic bacterial production showed a consistent positive response to warming across the AQUASHIFT studies (Figs. 2, 3), we argue therefore that both algal exudation and bacterial decomposition processes contributed to DOM accumulation during the AQUASHIFT phytoplankton blooms. In concert, a higher partitioning of organic carbon from the pool of particulate to dissolved matter appears to be a probable consequence of ocean warming.

Interestingly, both increasing daily light dose (AQ5) and copepod density (AQ6) had a contrary effect on $dcCHO_{slope}$ compared to warming, leading to a slower accumulation of dcCHO (Fig. 2). The significantly lower temperature response of $dcCHO_{slope}$ with decreasing copepod density during AQ6, likely also masking a potential temperature response (Fig. 2), may indicate an indirect effect of copepod density on DOC dynamics, as it has been shown that changes in grazer abundance can have a notable effect on bacterial activities by triggering a trophic cascade via ciliates and heterotrophic nanoflagellates (HNF; Zöllner et al. 2009). Thus, a decrease in copepod density may likely have relieved bacteria from direct grazing pressure by HNF, thereby enabling a more pronounced accumulation of dissolved organic carbon species at elevated temperature. Regarding the negative effect of increasing daily light dose on $dcCHO_{slope}$, the underlying mechanisms remain elusive, but it may be speculated that any potential changes in algal exudation through increased light availability may have been compensated by the enhanced bacterial carbon consumption due to the likely labile nature of freshly produced algal solutes.

TEP dynamics

In most of the experiments, a slight decrease in DOC and dcCHO was observed towards the end of the experimental period in the elevated temperature treatments, which closely coincided with changes in the concentration of TEP. Carbohydrates are known to be the precursor material and basic component of TEP. In general, two ways of TEP production have so far been reported, that is, the direct release of carbohydrate-rich cell surface material by phytoplankton cells and the abiotic aggregation of carbohydrate-containing components of the DOM pool (Chin et al. 1998; Engel et al. 2004). The TEP dynamics observed in the various AQUASHIFT experiments, in fact, indicate the presence of both TEP production mechanisms. During AQ5, the TEP dynamics showed a considerable and temperature-dependent increase in TEP already during bloom development, likely indicating an algal origin (Fig. 2). Similarly, a stimulation of TEP production and aggregation by rising temperature has been previously reported for various monoalgal cultures (Thornton and Thake 1998; Claquin et al. 2008). In AQ5, this first peak was followed by a decline in TEP under in situ temperature conditions, whereas the concentration further increased in the post-bloom phase of the elevated temperature treatments, thus yielding an overall significant temperature response (Table 5; Fig. 2). In contrast to AQ5, low and temperature-independent average concentrations of TEP were observed during the bloom of the experiments AQ2 and AQ6, followed by a steep increase in TEP during the late post-bloom phase of the elevated temperature treatments, which suggests a strengthened influence of either heterotrophic or abiotic processes. Several mesocosm and field studies (e.g., Passow and Alldredge 1995b; Engel 2004) have reported a strong potential of TEP to promote the aggregation and sinking of particulate matter to depth. This depends, however, critically on the timing and interplay of TEP production with other biological processes, such as microbial degradation and grazing. While a consistent positive trend of the post-bloom TEP dynamics in response to experimental warming was observed during the here presented AQUASHIFT studies (Fig. 3), its potential to influence the organic matter transport to depth via the biological pump remains uncertain due to the late timing of the event.

Organic matter elemental composition

Concerning the third hypothesis that warming would lead to a preferential remineralisation of phosphorus over carbon, thereby increasing their elemental ratios in POM and DOM, we cannot fully reject the null hypothesis. Only 1 of 4 studies showed an increase in particulate $C:P_{mean}$ with rising temperature (AQ 6). The effect was, however, slightly insignificant (Table 6; Fig. 2). In contrast, the other 3 studies displayed rather a decrease in $POC:POP_{mean}$, with a significant result in only 1 study (AQ3; Fig. 2). This decrease in the average ratio of POC to POP may, in fact, rather suggest a temperature-induced shift in the turnover dynamics of organic phosphorus compounds. Thus, results from an AQUASHIFT-related microcosm experiment have shown that experimental warming can substantially stimulate phosphorus cycling through the activity of the organic phosphorus-cleaving enzyme alkaline phosphatase (APA; Wohlers-Zöllner et al. 2011), hence enabling a faster replenishment of the POP pool at elevated temperature and reducing the C:P ratio of POM.

The average ratio of DOC to DOP did not show a significant response to any of the investigated environmental stressors (Fig. 2). In summary, the strong divergence in temperature patterns between studies impedes conclusions about the effects of ocean warming on POM and DOM elemental stoichiometry (Fig. 1).

Potential consequences for marine elemental cycling

One of the key drivers of biogeochemical cycling in the ocean is the biological carbon pump, which transports photosynthetically-bound carbon from the sunlit surface to deeper water layers. While most of the organic biomass is recycled back to carbon dioxide (CO_2) and other inorganic constituents on its way down, only the fraction that is transported below the winter-mixed layer actually contributes to the ocean's capacity to take up atmospheric CO_2. Ocean warming-mediated changes in the potential of the biological pump to transport carbon to depth, for instance through shifts in the partitioning of organic matter between its particulate and dissolved phases or in the elemental ratio of the produced biomass (Riebesell et al. 2007; Bellerby et al. 2008), may hence provide an important feedback mechanism to the climate system. In this context, a significant effect of experimental warming on the magnitude of POM and DOM build-up is also indicated by the results of the AQUASHIFT experiments (Figs. 2, 3). Concerning the latter, the enhanced and also accelerated accumulation of dissolved organic carbon compounds may shift pelagic ecosystems towards a microbial-dominated recycling system, thereby reducing the overall strength of the biological pump (Morán et al. 2006; Kim et al. 2011). To what extent the pronounced stimulation of heterotrophic microbial processes compared to autotrophic PP during AQUASHIFT (Figs. 2, 3) may lead to the build-up of a refractory DOC pool, hence contributing to the long-term storage of carbon in the marine biosphere (Jiao et al. 2010), is currently not predictable.

Conclusions

Despite the limited number of studies and treatment replicates, the AQUASHIFT experiments have provided important information on ocean warming effects on a range of biogeochemical parameters that directly or indirectly contribute to the ocean's mitigating role in Earth's climate system. A major outcome of these experiments is the substantial, yet often neglected, role of the microbial food web in the functioning and efficiency of the biological carbon pump. Moreover, our analysis provides an example for the strong potential for interactive synergistic or antagonistic effects of several environmental factors on major biogeochemical parameters. Based on this knowledge, there is an urgent need for further research on the interactive effects of environmental stressors on microbial elemental cycling under future ocean conditions and the potential for climate feedbacks.

Acknowledgments We would like to thank A. Ludwig, N. Händel and P. Fritsche for their technical assistance in sample preparation and analysis. All members of the Kiel AQUASHIFT-team are appreciated for their help during the experiments. We are particularly grateful to E. Zöllner and the anonymous reviewers for their comments on an earlier version of this manuscript. This work was supported by Deutsche Forschungsgemeinschaft (DFG) grant no. RI 598/2-3 to U. R. and A. E. and by the Helmholtz Association (contract no. HZ-NG-102 to A. E.).

References

Azam F (1998) Microbial control of oceanic carbon flux: the plot thickens. Science 280:694–696

Barnett TP, Pierce DW, AchutaRao KM, Gleckler PJ, Santer BD, Gregory JM, Washington WM (2005) Penetration of human-induced warming into the world's oceans. Science 309:284–287

Bellerby RGJ, Schulz KG, Riebesell U, Neill C, Nondal G, Johannessen T, Brown KR (2008) Marine ecosystem community carbon and nutrient uptake stoichiometry under varying ocean acidification during the PeECE III experiment. Biogeosciences 5:1517–1527

Bopp L, Monfray P, Aumont O, Dufresne J-L, Le Treut H, Madec G, Terray L, Orr JC (2001) Potential impact of climate change on marine export production. Glob Biogeochem Cycles 15:81–99

Boyd PW, Doney SC (2002) Modeling regional responses by marine pelagic ecosystems to global climate change. Geophys Res Lett 29:1806

Breithaupt P (2009) The impact of climate change on phytoplankton-bacterioplankton interactions. Dissertation, Christian-Albrechts-University, Kiel, Germany

Brock TD (1981) Calculating solar radiation for ecological models. Ecol Model 14:1–19

Chin WC, Orellana MV, Verdugo P (1998) Spontaneous assembly of marine dissolved organic matter into polymers. Nature 391:568–572

Claquin P, Probert I, Lefebvre S, Veron B (2008) Effects of temperature on photosynthetic parameters and TEP production in eight species of marine microalgae. Aquat Microb Ecol 51:1–11

Copin MG, Avril B (1993) Vertical distribution and temporal variation of dissolved organic carbon in the North-Western Mediterranean Sea. Deep-Sea Res I 40:1963–1972

Davison IR (1991) Environmental effects on algal photosynthesis: temperature. J Phycol 27:2–8

Edwards M, Richardson AJ (2004) Impact of climate change on marine pelagic phenology and trophic mismatch. Nature 430:881–884

Engel A (2004) Distribution of transparent exopolymer particles (TEP) in the northeast Atlantic Ocean and their potential significance for aggregation processes. Deep-Sea Res I 51:83–92

Engel A, Goldthwait S, Passow U, Alldredge AL (2002) Temporal decoupling of carbon and nitrogen dynamics in a mesocosm diatom bloom. Limnol Oceanogr 47:753–761

Engel A, Thoms S, Riebesell U, Rochelle-Newall E, Zondervan I (2004) Polysaccharide aggregation as a potential sink of marine dissolved organic carbon. Nature 428:929–932

Engel A, Händel N, Wohlers J, Lunau M, Grossart HP, Sommer U, Riebesell U (2011) Effects of sea surface warming on the production and composition of dissolved organic matter during phytoplankton blooms: results from a mesocosm study. J Plankt Res 33:357–372

Finkel ZV, Beardall J, Flynn KJ, Quigg A, Rees TAV, Raven JA (2009) Phytoplankton in a changing world: cell size and elemental stoichiometry. J Plankt Res 32:119–137

Fuhrman JA, Azam F (1982) Thymidine incorporation as a measure of heterotrophic bacterioplankton production in marine surface waters: evaluation and field results. Mar Biol 66:109–120

Gargas E (1975) A manual for phytoplankton primary production studies in the Baltic. Baltic Mar Biol 2:1–88

Hansen HP, Koroleff F (1999) Determination of nutrients. In: Grasshoff K, Kremling K, Ehrhardt M (eds) Methods of seawater analysis. Wiley VCH, Weinheim, pp 159–228

Jiao N, Herndl GJ, Hansell DA, Benner R, Kattner G, Wilhelm SW, Kirchman DL, Weinbauer MG, Luo T, Chen F, Azam F (2010) Microbial production of recalcitrant dissolved organic matter: long-term carbon storage in the global ocean. Nat Rev Microbiol 8:593–599

Kawasaki N, Benner R (2006) Bacterial release of dissolved organic matter during cell growth and decline: molecular origin and composition. Limnol Oceanogr 51:2170–2180

Kim JM, Lee K, Shin K, Yang EJ, Engel A, Karl DM, Kim HC (2011) Shifts in biogenic carbon flow from particulate to dissolved forms under high carbon dioxide and Warm Ocean conditions. Geophys Res Lett 38:L08612

Kroeker KJ, Kordas RL, Crim RN, Singh GG (2010) Meta-analysis reveals negative yet variable effects of ocean acidification on marine organisms. Ecol Lett. doi:10.1111/j.1461-0248.2010.01518x

Kujawinski EB (2011) The impact of microbial metabolism on marine dissolved organic matter. Annu Rev Mar Sci 3:567–599

Levitus S, Antonov J, Boyer T (2005) Warming of the world ocean, 1955–1998. Geophys Res Lett 32:L02604

Lewandowska AM, Sommer U (2010) Climate change and the spring bloom: a mesocosm study on the influence of light and temperature on phytoplankton and mesozooplankton. Mar Ecol Prog Ser 405:101–111

Lewandowska AM, Breithaupt P, Hillebrand H, Hoppe HG, Jürgens K, Sommer U (2011) Responses of primary productivity to increased temperature and phytoplankton diversity. J Sea Res. doi:10.1016/j.seares.2011.10.003

López-Urrutia A, San Martin E, Harris RP, Irigoien X (2006) Scaling the metabolic balance of the oceans. Proc Nat Acad Sci 103:8739–8744

Meehl GA, Stocker TF, Collins WD, Friedlingstein P, Gaye AT, Gregory JM, Kitoh A, Knutti R, Murphy JM, Noda A, Raper SCB, Watterson IG, Weaver AJ, Zhao ZC (2007) Global climate projections. In: Solomon S, Qin MMD, Chen Z, Marquis M, Averyt KB, Tignor M, Miller HL (eds) Climate change 2007: the physical science basis. Contribution of working group I to the fourth assessment report of the intergovernmental panel on climate change. Cambridge University Press, Cambridge, pp 747–845

Morán XAG, Sebastián M, Pedrós-Alió C, Estrada M (2006) Response of Southern Ocean phytoplankton and bacterioplankton production to short-term experimental warming. Limnol Oceanogr 51:1791–1800

Morán XAG, López-Urrutia A, Calvo-Díaz A, Li WKW (2010) Increasing importance of small phytoplankton in a warmer ocean. Glob Change Biol 16:1137–1144

Müren U, Berglund J, Samuelsson K, Andersson A (2005) Potential effects of elevated sea-water temperature on pelagic food webs. Hydrobiol 545:153–166

Myklestad S, Skånøy E, Hestmann S (1997) A sensitive and rapid method for analysis of dissolved mono- and polysaccharides in seawater. Mar Chem 56:279–286

Norrman B, Zweifel UL, Hopkinson CS, Fry B (1995) Production and utilization of dissolved organic carbon during an experimental diatom bloom. Limnol Oceanogr 40:898–907

O'Connor MI, Piehler MF, Leech DM, Anton A, Bruno JF (2009) Warming and resource availability shift food web structure and metabolism. PLoS Biol 7:e1000178. doi:10.1371/journal.pbio.1000178

Ogawa H, Amagai Y, Koike I, Kaiser K, Benner R (2001) Production of refractory dissolved organic matter by bacteria. Science 292:917–920

Passow U (2002) Transparent exopolymer particles (TEP) in aquatic environments. Prog Oceanogr 55:287–333

Passow U, Alldredge AL (1995a) A dye-binding assay for the spectrophotometric measurement of transparent exopolymer particles (TEP). Limnol Oceanogr 40:1326–1335

Passow U, Alldredge AL (1995b) Aggregation of a diatom bloom in a mesocosm: the role of transparent exopolymer particles (TEP). Deep-Sea Res II 42:99–109

Qian J, Mopper K (1996) Automated high-performance, high-temperature combustion total organic carbon analyzer. Analyt Chem 68:3090–3097

Redfield AC, Ketchum BM, Richards FA (1963) The influence of organism on the composition of sea-water. In: Hill MN (ed) The sea. Wiley, New York, pp 26–77

Riebesell U, Schulz KG, Bellerby RGJ, Botros M, Fritsche P, Meyerhöfer M, Neill C, Nondal G, Oschlies A, Wohlers J, Zöllner E (2007) Enhanced biological carbon consumption in a high CO_2 ocean. Nature 450:545–549

Riebesell U, Körtzinger A, Oschlies A (2009) Sensitivities of marine carbon fluxes to ocean change. Proc Nat Acad Sci 106:20602–20609

Sarmiento JL, Hughes TMC, Stouffer RJ, Manabe S (1998) Simulated response of the ocean carbon cycle to anthropogenic warming. Nature 393:245–249

Sarmiento JL, Slater R, Barber R, Bopp L, Doney SC, Hirst AC, Kleypas J, Matear R, Mikolajewicz U, Monfray P, Soldatov V, Spall SA, Stouffer R (2004) Response of ocean ecosystems to climate warming. Glob Biogeochem Cycles 18:GB3003

Schartau M, Engel A, Schröter J, Thoms S, Völker C, Wolf-Gladrow D (2007) Modelling carbon overconsumption and the formation of extracellular particulate organic carbon. Biogeosciences 4:433–454

Sharp JH (1974) Improved analysis for particulate organic carbon and nitrogen from seawater. Limnol Oceanogr 19:984–989

Sharples J, Ross ON, Scott BE, Greenstreet SPR, Fraser H (2006) Inter-annual variability in the timing of stratification and the spring bloom in the North-western North Sea. Cont Shelf Res 26:733–751

Siegenthaler U, Sarmiento JL (1993) Atmospheric carbon dioxide and the ocean. Nature 365:119–125

Simon M, Azam F (1989) Protein content and protein synthesis rates of planktonic marine bacteria. Mar Ecol Prog Ser 51:201–213

Sommer U, Lengfellner K (2008) Climate change and the timing, magnitude, and composition of the phytoplankton spring bloom. Glob Change Biol 14:1199–1208

Sommer U, Lewandowska A (2011) Climate change and the phytoplankton spring bloom: warming and overwintering zooplankton have similar effects on phytoplankton. Glob Change Biol 17:154–162

Sommer U, Aberle N, Engel A, Hansen T, Lengfellner K, Sandow M, Wohlers J, Zöllner E, Riebesell U (2007) An indoor mesocosm system to study the effect of climate change on the late winter

and spring succession of Baltic Sea phyto- and zooplankton. Oecologia 150:655–667

Steemann Nielsen E (1952) The use of radioactive carbon (14C) for measuring production in the sea. J Cons Int Explor Mer 18:117–140

Stoderegger K, Herndl GJ (1998) Production and release of bacterial capsular material and its subsequent utilization by marine bacterioplankton. Limnol Oceanogr 43:877–884

Thingstad TF, Hagström Å, Rassoulzadegan F (1997) Accumulation of degradable DOC in surface waters: is it caused by a malfunctioning microbial loop? Limnol Oceanogr 42:398–404

Thornton DCO, Thake B (1998) Effect of temperature on the aggregation of *Skeletonema costatum* (Bacillariophyceae) and the implication for carbon flux in coastal waters. Mar Ecol Prog Ser 174:223–231

Tilzer MM, Dubinsky Z (1986) Effects of temperature and day length on the mass balance of Antarctic phytoplankton. Polar Biol 7:35–42

Van den Meersche K, Middelburg JJ, Soetaert K, van Rijswijk P, Boschker HTS (2004) Carbon-nitrogen coupling and algal-bacterial interactions during an experimental bloom: modeling a ^{13}Ctracer experiment. Limnol Oceanogr 49:862–878

Verity PG (1981) Effects of temperature, irradiance, and daylength on the marine diatom Leptocylindrus danicus cleve. I. Photosynthesis and cellular composition. J Exp Mar Biol Ecol 55:79–91

Wiltshire KH, Manly BFJ (2004) The warming trend at Helgoland Roads, North Sea: phytoplankton response. Helgol Mar Res 58:269–273

Wohlers J (2009) The impact of climate change on phytoplankton-bacterioplankton interactions. Dissertation, Christian-Albrechts-University, Kiel, Germany

Wohlers J, Engel A, Zöllner E, Breithaupt P, Jürgens K, Hoppe HG, Sommer U, Riebesell U (2009) Changes in biogenic carbon flow in response to sea surface warming. Proc Nat Acad Sci 106:7067–7072

Wohlers-Zöllner J, Breithaupt P, Walther K, Jürgens K, Riebesell U (2011) Temperature and nutrient stoichiometry interactively modulate organic matter cycling in a pelagic algal–bacterial community. Limnol Oceanogr 56:599–610

Wolfstein K, Brouwer JFC, Stal LJ (2002) Biochemical partitioning of photosynthetically fixed carbon by benthic diatoms during short-term incubations at different irradiances. Mar Ecol Prog Ser 245:21–31

Zöllner E, Hoppe HG, Sommer U, Juergens K (2009) Effect of zooplankton-mediated trophic cascades on marine microbial food web components (bacteria, nanoflagellates, ciliates). Limnol Oceanogr 54:262–275